BUILDING SOFTWARE FOR ANALYZING MUCK PILES AFTER BLASTING IN LABORATORY CONDITIONS WITH INTEGRATED ARTIFICIAL INTELLIGENCE

Tung Lam Vu[1,*], Manh Tung Vu[2], Trong Hieu Vu[1], Van Lam Nguyen[3]

[1]*Institute of Techniques for Special Engineering, Le Quy Don Technical University*

[2]*People's Police College 1*

[3]*Naval Technical Institute*

Abstract

In the mining and tunneling industry, the mean particle size (D_{tb}) of a muck pile after blasting is a key parameter for evaluating blasting efficiency. Numerous solutions exist for determining mean particle size by photographing muck piles after blasting using commercial software such as Split-Desktop and WipFrag, but these incur annual costs of thousands of US dollars. To address this limitation, the study develops software that analyzes images of muck piles after blasting, providing Swebrec, Gate-Gaudin-Schumann, and Rosin-Rammler particle size distribution (PSD) functions and their corresponding mean particle sizes. The software utilizes open-source resources and integrates the SAM2 artificial intelligence model to facilitate editing of each rock fragment detected in the image. The software's mean particle size results are compared with those from traditional sieving analysis, with differences ranging from 5% to 7% for image segmentation data. These results demonstrate the software's feasibility as a low-cost, reliable alternative to the sieving process.

Keywords: *Rock fragmentation; particle size distribution (PSD); Swebrec function; Gate-Gaudin-Schumann function; Rosin-Rammler function; SAM2; comminution; mean particle size (D_{tb}); blasting.*

1. Introduction

In the blasting work, especially in open-pit mines and tunneling excavation, fragmenting a muck pile after an explosion plays a vital role because it affects transport, comminution costs, and subsequent processes [1], [2]. In the past, traditional methods were only direct observation of a muck pile and sieve analysis. Several studies used traditional sieve analysis, such as the studies of the author D. T. Thang *et al.* [3]-[6] figured out relations between various factors on the mean particle size D_{tb}, this was always a crucial parameter, representing influences of an explosion. Significantly, the study of the author V. T. Lam *et al.* [7] contributed a method directly determining Swebrec

* Corresponding author, email: lamvt@lqdtu.edu.vn
DOI: 10.56651/lqdtu.jst.v8.n01.970.sce

distribution functions based on experimental data from sieve analysis. Along with that, it did not require prerequisite knowledge for complex machine learning techniques and statistical theories.

However, when using this traditional method, the accuracy depends on the number and the size of sieves, it is incompatible with a large product industry since the method consumes a lot of time, leading to a stagnant process. According to the development of technology, applying automation in image analysis helps reduce manpower and time, as well as providing quantitative data for optimizing the blasting process. Using image processing techniques for rock fragmentation has been widely discussed since the '90s of the last century [8], [9].

Image processing techniques are usually divided into two big groups. In the first group, authors use algorithms such as segmentation and edge detection based on watershed [10]-[12] to analyze photos of muck piles. This approach requires a deep knowledge of programming and computer vision often preferred by computer scientists. In the second group, authors use software currently existing in the market, such as Split-Desktop, Wipfrag, or MetricsManager^{TM} Pro web-based platform [13]-[15] to fragment muck piles through images, drawing some correction factors for errors because the software often does not detect fine-grain size in detail. Although commercial softwares have noticeable performance that can be considered to become an alternative to traditional sieve analysis, they cost thousands of US dollars per year for use, making them hard to be approached by developing countries.

Moreover, thanks to the robust development of artificial intelligence in recent years, one new approach is gradually increasing, which is to combine open-source artificial intelligence models to analyze a muck pile after blasting such as CNN, ResNet, U-CARFnet, and SAM [16]-[19], reaching remarkable results without requiring too deep programming skills, it is likely suitable for earth scientists who have a little programming knowledge.

In Vietnam, studying and using image processing techniques in rock fragmentation is not very much, the author H. N. Duc [20] proposed an automatic method for determining the gradation of stone aggregates. However, the experimental environment consists of all coarse grains, far apart on a white background with visual boundaries of rock particles, which are unsuitable for both practice and experiment.

Hence, this paper studies to establish a new software based on integrating an artificial intelligence SAM2 of META AI [21] to fragment a muck pile after blasting. Some photos of muck piles in experimental conditions are then taken and turned into the input of this software. The outputs are rock particle size distributions according to three well-known functions, such as Swebrec, Gate-Gaudin-Schumann, and Rosin-Rammler, with their corresponding mean particle size D_{tb} for each function. Values of D_{tb} are calculated by the software with both data from the image segmentation process and data from the sieving procedure are compared with each other. These results are then compared to D_{tb} values of traditional sieve analysis, errors fluctuate from 5% to 7% for image segmentation data, showing the reliability of the software.

2. Experimental study

2.1. Experimental model

The experimental model is set up to capture all the fragments of the specimen after detonation, ensuring no secondary rock breaking. The experimental model is described in detail as follows:

The specimens used in experiments have the shape of (15×15×15) cm, which are made of coral concrete and reach the grade M250 (B20). The aggregate for one cubic meter is shown in Tab. 1.

Tab. 1. Summary table of aggregate for one cubic meter

Cement PCB40 (kg)	Coral stone (2×4) cm (m^3)	Coral stone (1×2) cm (m^3)	Coral sand (m^3)	Water (liter)	Proportion water/cement	Slump (cm)
440	0.5	0.15	0.5	272.8	0.62	6

The specimen is placed on a wooden sheet, covered by half of an empty steel barrel, which has a diameter of 55 cm. The inner surface of the barrel is arranged to be covered with a layer of 3 cm-thick foam material to ensure that the flying rocks would not be secondary broken. A heavy object is placed on the top of the barrel to ensure that the barrel would not bounce when detonated, causing the fragments to be thrown outside the range of the barrel. The explosive used in the experiments is the No. 8 electrical fuse, equivalent to 1 g of TNT, placed in the center of the specimen, the blasting machine is MFB-200 from China. The experimental model is shown in Fig. 1a, and all experimental steps in sequence in the field are shown in Fig. 1b to 1f.

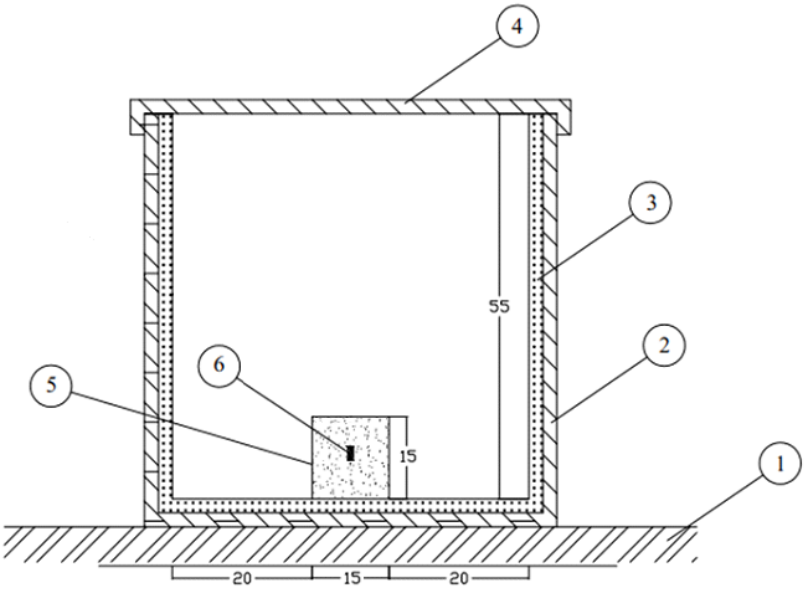

(a)

(b)

(c)

(d)

(e)

(f)

(g)

Fig. 1. Experimental model (a) and actual photos in the field (b, c, d, e, f, g)

1 - wooden sheet; 2 - barrel wall; 3 - foam material;

4 - heavy object; 5 - specimen; 6 - No. 8 electrical fuse.

Three typical experiments are carried out, corresponding to three different sunlight conditions. Taking photos with a digital camera having a resolution of 12 MP, the results after blasting are shown in Fig. 2.

(a) *(b)* *(c)*

Fig. 2. Experiment results.

In Fig. 2, various sunlight conditions correspond to Figs. 2a, 2b, 2c are intense sunlight, gentle sunlight, and overcast conditions, respectively. The results shown in Figs. 2a, 2b, 2c indicate that blasting products are clear discrete fragments, with very few and almost no fragments flying out of the steel barrel coverage, ensuring the collection of the entire blasting products, and validating the accuracy of the experimental model. A ruler is placed in the final image to serve as a tool to fine-tune the scale of fragmentation results in the image processing step.

2.2. Raw experimental data collection

To ensure the accuracy of rock fragmentation by image processing, the paper collects raw experimental data by the traditional sieving method, as a basis for comparison with the final results. Blasting products are analyzed by sieves with sizes of 2.5, 5, 10, 20, 30, 40, 50, and 60 (mm), respectively, obtaining 9 groups of average particle size following sieve size. Each group is then weighed, and information is summarized as a cumulative weight percentage. The data of 3 typical samples is listed in Tab. 2, with the medium size of the sieve greater than 60 mm varying based on the maximum size of the particle obtained from the software.

Tab. 2. The table of cumulative weight percentage

No.	**Sieve sizes *x*, mm**								
	< 2.5	**2.5-5**	**5-10**	**10-20**	**20-30**	**30-40**	**40-50**	**50-60**	**> 60**
	1.25	**3.75**	**7.50**	**15**	**25**	**35**	**45**	**55**	**Varies**
1	0.0178	0.0325	0.0625	0.1190	0.1887	0.3239	0.4035	0.5654	1.0000
2	0.0236	0.0442	0.0868	0.1585	0.2785	0.4118	0.5946	0.7004	1.0000
3	0.0191	0.0386	0.0796	0.1490	0.2248	0.3200	0.5717	0.6880	1.0000

3. Building software for rock fragmentation after blasting

Based on the open-source artificial intelligence SAM2 from META AI [21], this paper builds new software to fragment a muck pile after blasting. The fragments of data obtained from the software are then turned into the input of the direct analysis method, which was proposed by V. T. Lam *et al.* [7], drawing particle size distributions and their mean particle sizes. The software has the name "Rock Segmentation", and the general interface of the software is as follows:

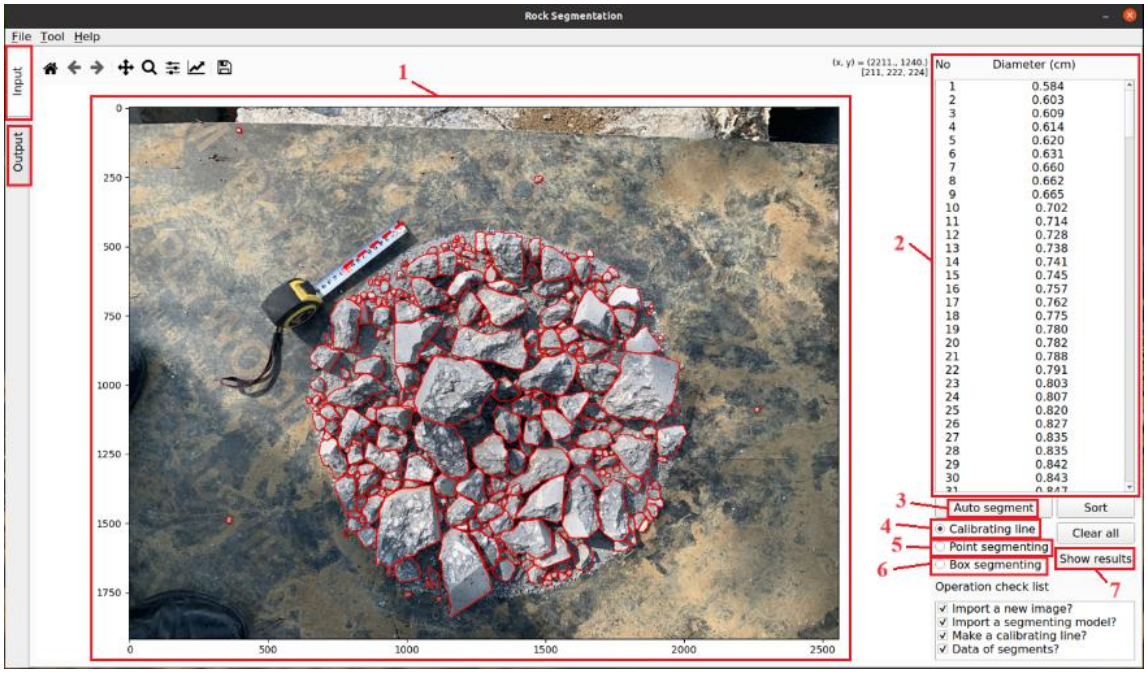

Fig. 3. The general interface of the Rock Segmentation software.

In Fig. 3, the main interface for using this software consists of an Input tab and an Output tab. The Input tab includes: {1} is the interactive interface showing the image of a muck pile and detected fragments, {2} is the table listing data of detected fragments, {3} is the auto-detect function, {4} is the function of establishing a dimension reference line (shown in the red dashed line on the ruler), {5} is the function detecting a fragment as a point of mouse click, {6} is the function detecting a fragment in a selected rectangular region, {7} is the function displaying results under the graph of particle size distribution functions according to three functional form such as Swebrec, Gate-Gaudin-Schumann, and Rosin-Rammler, this function automatically actives the software to switch to the Output tab.

The software is written entirely in Python 3, combining programming techniques to make the open-source artificial intelligence model SAM2 work on a personal computer.

To save time in image analysis, the software is built on the Linux-based operating system Ubuntu 20.04 LTS to maximize the processing power of the Nvidia GTX 1660 Ti graphics card with the CUDA parallel computing library. The software can fragment a muck pile after blasting, including the following main functions:

Import data: import a muck pile photo after blasting as the ubiquitous image formats.

Export data: export data into 2 forms. Firstly, the image of a fragmented muck pile with red boundaries under the ubiquitous image formats. Secondly, a binary file with the extension *.prs contains data of the original image and its detected fragments.

Display: the software can display the results as an image of a muck pile after blasting, with each detected fragment clearly observed and information on its average diameter, combined with interactive and editable abilities. Moreover, the graph of particle size distribution functions in three forms, such as Swebrec, Gate-Gaudin-Schumann, Rosin-Rammler, and mean particle sizes, is shown in the Output tab of the software.

Functions: the software utilizes mechanisms of the SAM2 model, such as zero-shot, point prompt, and box prompt, to automatically produce editable results of each fragment. Besides, the software can detect fragments in the desired area instead of the entire image, which has not been available in any previous commercial softwares.

Generally speaking, the software produces the results as an image of a muck pile after blasting with clearly fragmented fragments. All parameters of the contour and area of fragments are saved as a file with extension *.prs of the software for later editing and upgrading of the model, thanks to the upgradable ability of SAM2. The software also allows reading results of particle size distribution graphs according to 3 famous functional forms, such as Swebrec, Gate-Gaudin-Schumann, and Rosin-Rammler functions, and their mean particle size D_{tb}.

4. Methodology determines PSDs and the mean particle size

This paper proposes methodologies for determining particle size distributions in the form of three well-known distribution functions, such as Swebrec, Gate-Gaudin-Schumann, and Rosin-Rammler, with data obtained from the aforementioned Rock Segmentation software.

4.1. Determining the Swebrec particle size distribution function and its mean particle size D_{tb}

Based on the methodology of the author V. T. Lam *et al.* [7], this paper also draws the equation directly determining the particle size distribution in Swebrec form. However, instead of taking data from the sieving process, this study takes data as fragmented fragments obtained from the aforementioned Rock Segmentation software.

The Swebrec function illustrating particle size distribution of a muck pile after blasting has the form as follows:

$$P = \frac{1}{1+\left[\frac{\ln\left(x_{\max}/x\right)}{\ln\left(x_{\max}/x_{50}\right)}\right]^{b}} \tag{1}$$

where P is the cumulative distribution of fragment size; x is the diameter of segmented fragment from Rock Segmentation software; x_{50} is the median or size of 50% passing for which $P(x_{50}) = 0.5$; $x_{\max}$ is the largest diameter of fragment size (mm) obtained from the software.

Employing Eq. (1) for a finite series of fragments obtained from the Rock Segmentation software, drawing the exponential coefficient b of the Swebrec particle size distribution as a unique solution of the analytical equation below:

$$\sum_{i=1}^{m}\frac{P_i\bar{\bar{x}}_i^{\,b}\ln\left(\bar{\bar{x}}_i+\varepsilon\right)}{\left(1+\bar{\bar{x}}_i^{\,b}\right)^2}-\sum_{i=1}^{m}\frac{\bar{\bar{x}}_i^{\,b}\ln\left(\bar{\bar{x}}_i+\varepsilon\right)}{\left(1+\bar{\bar{x}}_i^{\,b}\right)^3}=0 \text{ with } \bar{\bar{x}}_i=\frac{\ln\left[\left(x_{\max}+\varepsilon\right)/\left(x_i+\varepsilon\right)\right]}{\ln\left(x_{\max}/x_{50}\right)} \tag{2}$$

where P_i is cumulative distribution up to i^{th} fragment size from the software; $x_{\max}$, x_{50} is similar to equation (2); b is the exponential coefficient of the Swebrec function; m is the total fragment size obtained from the software (including size 0); ε is an infinitesimal number.

The mean particle size D_{tb} is the mathematical expectation of the particle size x. For data obtained from the software, D_{tb} can be calculated under the following equation:

$$D_{tb}=\int_0^1 x\,d\left[P_{(x)}\right]=\int_0^{x_{\max}} xp_{(x)}dx=D_{tb}=\int_0^{x_{\max}}\frac{b\ln^b\left(x_{\max}/x_{50}\right)\ln^{b-1}\left(x_{\max}/x\right)}{\left[\ln^b\left(x_{\max}/x_{50}\right)+\ln^b\left(x_{\max}/x\right)\right]^2}dx$$

$$=\sum_{i=1}^{iter}\frac{b\ln^b\left(x_{\max}/x_{50}\right)\ln^{b-1}\left(x_{\max}/\left(x_i+\varepsilon\right)\right)}{\left[\ln^b\left(x_{\max}/x_{50}\right)+\ln^b\left(x_{\max}/\left(x_i+\varepsilon\right)\right)\right]^2}\Delta x \text{ with } \Delta x=x_{\max}/iter \tag{3}$$

To modify for better results of D_{tb} values calculated from Swebrec PSD and that from traditional sieve analysis, this paper proposes to use Eq. (3') instead of Eq. (3) as follows:

$$D_{tb}=\sum_{i=1}^{iter}\frac{b\ln^b\left(x_{\max}/x_{58}\right)\ln^{b-1}\left(x_{\max}/\left(x_i+\varepsilon\right)\right)}{\left[\ln^b\left(x_{\max}/x_{58}\right)+\ln^b\left(x_{\max}/\left(x_i+\varepsilon\right)\right)\right]^2}\Delta x \text{ with } \Delta x=x_{\max}/iter \tag{3'}$$

where D_{tb} is the mean particle size (mm); x is particle size (mm); x_{max} is the largest particle size; $P(x)$ is Swebrec PSD function obtained from Eq. (1); $p(x)$ is probability distribution

of particle size x, obtained by partial derivative $P(x)$ for x; b is exponential coefficient of Swebrec PSD; ε is an infinitesimal number; *iter* is iteration number, chosen *iter* = 1000000; x_{58} is the median or size of 58% passing for which $P(x_{58}) = 0.58$.

4.2. Determining the Gate-Gaudin-Schumann particle size distribution function and its mean particle size D_{tb}

The Gate-Gaudin-Schumann function illustrating particle size distribution of a muck pile after blasting has the form as follows:

$$P = \left(\frac{x}{x_{\max}} \right)^a \tag{4}$$

where P is the cumulative distribution of fragment size; x is the diameter of a segmented fragment from Rock Segmentation software; $x_{\max}$ is the largest diameter of fragment size (mm) obtained from the software.

Employing the optimization of a loss function used in the material [7], it is simple to derive an analytical equation directly calculating the exponential coefficient a of the Gate-Gaudin-Schumann particle size distribution, which is compatible with the Rock Segmentation software as follows:

$$\sum_{i=1}^{m} P_i \overline{x}_i^a \ln\left(\overline{x}_i + \varepsilon\right) - \sum_{i=1}^{m} \overline{x}_i^{2a} \ln\left(\overline{x}_i + \varepsilon\right) = 0 \text{ with } \overline{x}_i = \frac{x_i}{x_{\max}} \tag{5}$$

where P_i is cumulative distribution up to i^{th} fragment size from the software; $x_{\max}$ is similar to equation (4); a is the exponential coefficient of the Gate-Gaudin-Schumann function; m is the total fragment size obtained from the software (including size 0); ε is an infinitesimal number.

D_{tb} can be calculated by the following equation, using fragment data from the software:

$$D_{tb} = \int_0^1 x d\left[P_{(x)}\right] = \int_0^{x_{\max}} x p_{(x)} dx = \int_0^{x_{\max}} x \frac{a x^{a-1}}{x_{\max}^a} dx = \int_0^{x_{\max}} \frac{a x^a}{x_{\max}^a} dx$$

$$= \frac{a x_{\max}}{a+1} \approx \sum_{i=1}^{iter} \frac{a x_i^a}{x_{\max}^a} \Delta x \text{ with } \Delta x = x_{\max} / iter \tag{6}$$

where D_{tb} is the mean particle size (mm); x is particle size (mm); x_{max} is the largest particle size; $P(x)$ is Gate-Gaudin-Schumann PSD function obtained from Eq. (4); $p(x)$ is probability distribution of particle size x, obtained by partial derivative $P(x)$ for x; a is exponential coefficient of Gate-Gaudin-Schumann PSD; ε is an infinitesimal number; *iter* is iteration number, chosen *iter* = 1000000.

4.3. Determining the Rosin-Rammler particle size distribution function and its mean particle size D_{tb}

The Rosin-Rammler function illustrating particle size distribution of a muck pile after blasting has the form as follows:

$$P = 1 - e^{-\left(\frac{x}{x_{63.2}}\right)^c} \tag{7}$$

where P is the cumulative distribution of fragment size; x is the diameter of a segmented fragment from Rock Segmentation software; $x_{63.2}$ is the median or size of 63.2% passing for which $P(x_{63.2}) = 0.632$.

Similarly, employing the optimization of a loss function used in the material [7], it is simple to derive an analytical equation directly calculating the exponential coefficient c of Rosin-Rammler particle size distribution, which is compatible with the Rock Segmentation software as follows:

$$\sum_{i=1}^{m} \frac{P_i \hat{x}_i^c \ln\left(\hat{x}_i + \varepsilon\right)}{e^{\hat{x}_i^c}} + \sum_{i=1}^{m} \frac{\hat{x}_i^c \ln\left(\hat{x}_i + \varepsilon\right)}{e^{\hat{x}_i^{2c}}} - \sum_{i=1}^{m} \frac{\hat{x}_i^c \ln\left(\hat{x}_i + \varepsilon\right)}{e^{\hat{x}_i^c}} = 0 \text{ with } \hat{x}_i = \frac{x_i}{x_{63.2}} \tag{8}$$

where P_i is cumulative distribution up to i^{th} fragment size from the software; $x_{63.2}$ is similar to equation (7); c is the exponential coefficient of the Rosin-Rammler function; m is the total fragment size obtained from the software (including size 0); ε is an infinitesimal number.

D_{tb} can be calculated by the following equation, using fragment data from the software:

$$D_{tb} = \int_0^1 x d\left[P_{(x)}\right] = \int_0^\infty x p_{(x)} dx = D_{tb} = \int_0^\infty x \frac{b x^{b-1}}{e^{\left(\frac{x}{x_{63,2}}\right)^b} x_{63.2}^b} dx = \int_0^\infty \frac{b x^b}{e^{\left(\frac{x}{x_{63,2}}\right)^b} x_{63.2}^b} dx$$

$$\approx \sum_{i=1}^{iter} \frac{b x_i^b}{e^{\left(\frac{x_i}{x_{63.2}}\right)^b} x_{63.2}^b} \Delta x \text{ with } \Delta x = \overline{x_{\max}} / iter \tag{9}$$

where D_{tb} is the mean particle size (mm); x is particle size (mm); $\overline{x_{\max}}$ is the largest particle size, reaching infinity for the Rosin-Rammler function, only choose $\overline{x_{\max}}$ = 200 (mm); $P(x)$ is Rosin-Rammler PSD function obtained from Eq. (7); $p(x)$ is probability distribution of particle size x, obtained by partial derivative $P(x)$ for x; c is exponential coefficient of Rosin-Rammler PSD; ε is an infinitesimal number; *iter* is iteration number, chosen *iter* = 1000000.

5. Results and analysis

The Rock Segmentation software exports the results in the form of an image, the particle size distribution graphs under three forms, such as Swebrec (SS-image), Gate-Gaudin-Schumann (GGS-image), Rosin-Rammler (RR-image), and D_{tb} values corresponding to 3 typical experiments with intense sunlight, gentle sunlight, and overcast conditions, respectively. Combined with comparisons to values of the sieving process (SS-sieve, GGS-sieve, and RR-sieve), the final results are shown in Figs. 4-6.

In Figs. 4-6, the lines GGS-image, RR-image, and SS-image are particle size distribution graphs under the form of Gate-Gaudin-Schumann, Rosin-Rammler, and Swebrec functions, respectively, following the input data from the Rock Segmentation software. Meanwhile, the lines GGS-sieve, RR-sieve, and SS-sieve are also particle size distribution graphs under the form of Gate-Gaudin-Schumann, Rosin-Rammler, and Swebrec functions, respectively, but following the input data from the sieve analysis. All the particle size distributions and the mean particle sizes are calculated via Eqs. (1)-(9). The final results are listed in Tabs. 3, 4.

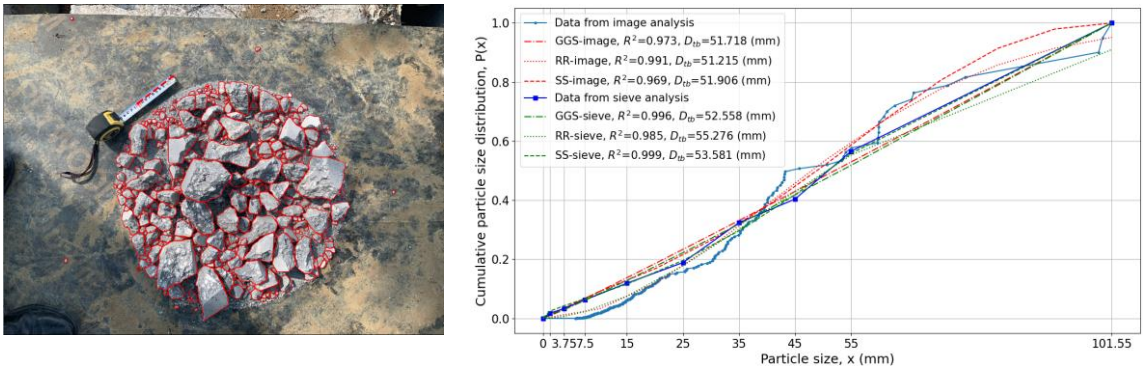

(a) *(b)*

Fig. 4. The result of the image analysis for experiment No. 1.

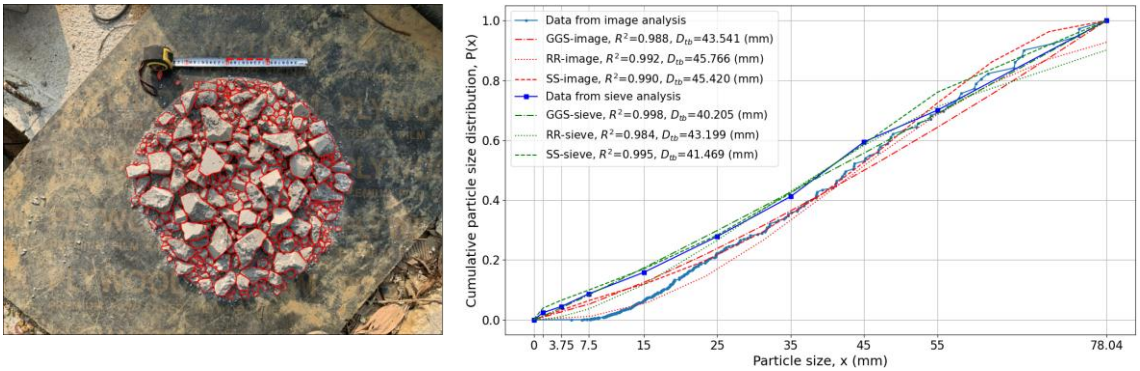

(a) *(b)*

Fig. 5. The result of the image analysis for experiment No. 2.

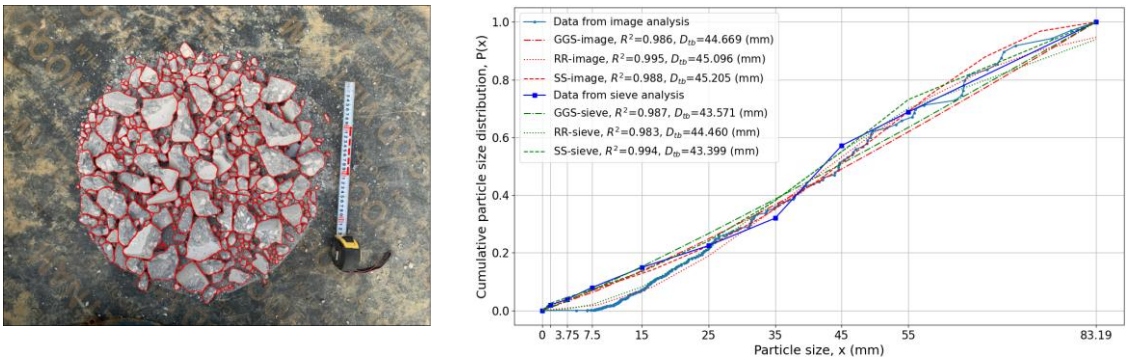

(a) *(b)*

Fig. 6. The result of the image analysis for experiment No. 3.

Tab. 3. Summary table between D_{tb} values calculated from PSD applying for sieve and image data, compared to those from traditional sieve analysis

STT	D_{tb} from GGS (mm)		D_{tb} from RR (mm)		D_{tb} from Swebrec (mm)		D_{tb} from sieve analysis
	GGS-image	GGS-sieve	RR-image	RR-sieve	SS-image	SS-sieve	
1	51.826	52.614	51.321	55.309	52.014	53.606	54.880
	5.56%	4.13%	6.49%	0.78%	5.22%	2.32%	
2	43.563	40.213	45.789	43.200	45.443	41.474	47.181
	7.67%	14.77%	2.95%	8.44%	3.68%	12.10%	
3	44.640	43.559	45.067	44.459	45.175	43.394	49.355
	9.55%	11.74%	8.69%	9.92%	8.47%	12.08%	
Average	7.60%	10.21%	6.04%	6.38%	5.79%	8.83%	

Tab. 4. Summary and comparison table between D_{tb} values from PSD applying for sieve data and image data

No.	D_{tb} from Gate-Gaudin-Schumann (mm)			D_{tb} from Rosin-Rammler (mm)			D_{tb} from Swebrec (mm)		
	GGS-image	GGS-sieve	Differ	RR-image	RR-sieve	Differ	SS-image	SS-sieve	Differ
1	51.826	52.614	1.50%	51.321	55.309	7.21%	52.014	53.606	2.97%
2	43.563	40.213	8.33%	45.789	43.200	5.99%	45.443	41.474	9.57%
3	44.640	43.559	2.48%	45.067	44.459	1.37%	45.175	43.394	4.10%
	Average		4.10%	Average		4.86%	Average		5.55%

From Figs. 4-6, and Tabs. 3, 4, it can be seen that all particle size distribution functions have coefficients of determination R^2 greater than 0.97, proving that they fit well with not only the data of sieve analysis, but also the data of image analysis. Tab. 3 shows that all errors of D_{tb} calculated from PSDs and those from traditional sieve analysis are smaller than 10%. The results of image analysis from the software with suffixes

"-image" always have errors smaller than the results of sieve analysis with suffixes "-sieve", corresponding to 7.6% and 10.21% for GGS function, 6.04% and 6.38% for RR function, 5.79% and 8.83% for Swebrec function. These results prove the reliability of the software when its results are close to traditional sieve analysis.

Quantitatively analyzing Tab. 4 shows that the condition of input images is one of factors impacting on accuracy of the software. Images with intense sunlight and overcast conditions have small errors, differences are only about 1% for both GGS and Swebrec PSDs. For the image with gentle sunlight condition, the errors compared to the two remaining sunlight conditions are higher for all three PSDs, fluctuating between 5% to 6%. By directly observing, it can be seen that the color scale of this image is inclined to be yellowish because of the post-processing procedure by a digital camera, which is the reason leading to lower accuracy of the software. The shadow due to various sunlight intensities does not affect segmentation results of the software, because differences between intense sunlight and overcast condition are only about 1%. Hence, one conclusion can be drawn that input images for the software should be original format, meaning the raw file according to photography perspective.

Besides, the results from Tab. 4 also show the flexibility of Eqs. (1)-(9) when they are successfully applied for both sieve data (with a small amount of data, corresponding to a number of average sieve sizes) and image analysis data (with a large amount of data, corresponding to all detected segments). Average errors fluctuates from just over 4% to about 5%, showing the reliability of the results.

6. Conclusion and recommendation

The mean particle size of a muck pile after blasting is a key parameter for evaluating blasting efficiency. This study developed software integrating the SAM2 artificial intelligence model to segment muck pile fragments after blasting and calculate mean particle size values from images. Additionally, each detected fragment can be editable and stored in a binary file with a specified extension for updatable purposes in the future. Analysis of the mean particle size D_{tb} from the software shows that results from image segmentation and those from sieving differ on average by less than 10%. When compared, average errors range from 4% to 5%.

The software can be considered to replace the manual sieving process, which takes a lot of time and effort, at least in laboratory conditions with adequate lighting, no dust, and clear images. This software can also be considered an alternative to commercial software currently on the market, such as Split-Desktop and Wipfrag, which cost thousands of US dollars per year to use, not suitable for developing countries.

Recommendation: While the software has only demonstrated its efficiency under controlled laboratory conditions, with adequate lighting, no dust, and precisely conducted sieving, it shows potential for maintaining accuracy in real-world production, provided that the dataset is expanded. This is also the basis for enhancing the zero-shot function of the artificial intelligence model in the software. In addition, because the software is built on an open-source Linux-based operating system, it can be further developed to integrate into portable camera hardware, which can directly capture images and export results on the field, helping speed up efficiency and progress construction.

References

[1] H. S. Giao và nnk, *Nổ hóa học lý thuyết và thực tiễn*. Nxb Khoa học tự nhiên và Công nghệ, 2010.

[2] Đ. T. Thắng và nnk, *Nổ mìn trong ngành mỏ và công trình*. Nxb Khoa học tự nhiên và Công nghệ, 2015.

[3] Đ. T. Thắng và nnk, "Nghiên cứu ảnh hưởng của hình dạng lượng nổ đến mức độ đập vỡ đất đá bằng phương pháp thực nghiệm", *Tạp chí Khoa học và Kỹ thuật*, Vol. 13, No. 04, tr. 113-121, 2018.

[4] D. T. Thang *et al.*, "Study on the reasonable parameters of the cylinder shaped charge with tapered liner funnel to destroy stone", *ISRM International Symposium on Rock Mechanics and Engineering for Sustainable Energy*, Hanoi, Vietnam, 2019. ISRM-VCRES-2019-010

[5] D. T. Thang *et al.*, "Study on the reasonable parameters of the concentric hemisphere-style shaped charge for destroying rock", *International Conference on Innovations for Sustainable and Responsible Mining*, Hanoi, Vietnam, 2020. DOI: 10.1007/978-3-030-60839-2_3

[6] Д. Ч. Тханг и др., "Исследования действия кумулятивных зарядов с выемкой полусферической эксцентрической формы для разрушения горных пород", *Журнал Устойчивое развитие горных территорий*, Т.13, №2, с. 281-291, 2021. DOI: 10.21177/1998-4502-2021-13-2-281-291

[7] V. T. Lam *et al.*, "An approach to determine and predict the mean particle size of a muck pile after blasting according to Swebrec particle size distribution law based on the form of single spherical charge in laboratory scale", *Journal of Science and Technique - Section on Special Construction Engineering*, Vol. 07, No. 02, pp. 21-34, 2024. DOI: 10.56651/lqdtu.jst.v7.n02.879.sce

[8] G. C. Hunter *et al.*, "A review of image analysis techniques for measuring blast fragmentation", *Mining Science and Technology*, Vol. 11, pp. 19-35, 1990.

[9] J. M. Kemeny *et al.*, "Analysis of rock fragmentation using digital image processing", *Journal of Geotechnical Engineering*, Vol. 119, pp. 1144-1160, 1993.

[10] W. Wang *et al.*, "A delineation algorithm for particle images online", *Communications in Computer and Information Science*, Vol. 14, Springer, Berlin, Heidelberg, MCO 2008. DOI: 10.1007/978-3-540-87477-5_50

[11] A. Amankwah and C. Aldrich, "Rock image segmentation using watershed with shape markers", *Proceedings of Applied Imagery Pattern Recognition Workshop (AIPR)*, 2010. DOI: 10.1109/AIPR.2010.5759719

[12] Q. Guo *et al.*, "A method of blasted rock image segmentation based on improved watershed algorithm", *Scientific Reports*, Vol. 12, 7143, 2022. DOI: 10.1038/s41598-022-11351-0

[13] S. Nanda and B. K. Pal, "Analysis of blast fragmentation using wipfrag", *International Journal of Innovative Science and Research Technology*, Vol. 5, Iss. 6, Jun. 2020. DOI: 10.38124/IJISRT20JUN1086

[14] A. Saadoun *et al.*, "Fragmentation analysis using digital image processing and empirical model (KuzRam) a comparative study", *Journal of Mining Institute*, Vol. 257, pp. 822-832, 2022. DOI: 10.31897/PMI.2022.84

[15] J. Figueiredo *et al.*, "Blasting fragmentation study using 3D image analysis of a hard rock mine", *Applied Sciences*, Vol. 13(12), 7090, 2023. DOI: 10.3390/app13127090

[16] T. Bamford *et al.*, "A deep learning approach for rock fragmentation analysis", *International Journal of Rock Mechanics and Mining Sciences*, Vol. 145, 2021. DOI: 10.1016/j.ijrmms.2021.104839

[17] C. Jin *et al.*, "Study on segmentation of blasting fragment images from open-pit mine based on U-CARFnet", *PLoS ONE*, Vol. 18(9), 2023. DOI: 10.1371/journal.pone.0291115

[18] Z. Ma *et al.*, "Zero-Shot Digital Rock Image Segmentation with a Fine-Tuned Segment Anything Model", *arXiv*:2311.10865. DOI: 10.48550/arXiv.2311.10865

[19] J. Zhao *et al.*, "Identification of Rock Fragments after Blasting by using deep learning-based segment anything model", *Minerals*, Vol. 14, 2024. DOI: 10.3390/min14070654

[20] H. N. Duc *et al.*, "Image processing-based automatic gradation of stone aggregates", *DTU Journal of Science and Technology*, Vol. 5(54), pp. 37-42, 2022.

[21] N. Ravi *et al.*, "SAM 2: Segment anything in images and videos", *arXiv*:2408.00714. DOI: 10.48550/arXiv.2408.00714

XÂY DỰNG PHẦN MỀM PHÂN TÍCH ĐỐNG ĐÁ SAU NỔ TRONG ĐIỀU KIỆN PHÒNG THÍ NGHIỆM TÍCH HỢP TRÍ TUỆ NHÂN TẠO

Vũ Tùng Lâm[1], Vũ Mạnh Tùng[2], Vũ Trọng Hiếu[1], Nguyễn Văn Lãm[3]

[1]*Viện Kỹ thuật công trình đặc biệt, Trường Đại học Kỹ thuật Lê Quý Đôn*

[2]*Trường Cao đẳng Cảnh sát nhân dân 1*

[3]*Viện Kỹ thuật Hải quân*

Tóm tắt: Trong ngành khai khoáng và đào hầm, cỡ hạt trung bình của đống đá sau nổ mìn là một thông số tổng hợp chính để đánh giá hiệu quả nổ mìn. Trên thế giới, có nhiều giải pháp cung cấp thông tin về cỡ hạt trung bình bằng cách chụp hình ảnh đống đá sau nổ mìn thông qua các phần mềm thương mại như Split-Desktop và WipFrag, nhưng chúng có chi phí hàng nghìn đô la Mỹ mỗi năm để sử dụng. Để giải quyết hạn chế này, bài báo xây dựng một phần mềm có chức năng phân tích ảnh chụp đống đá sau nổ, đưa ra thông tin về dạng hàm phân phối cỡ hạt Swebrec, Gate-Gaudin-Schumann, Rosin-Rammler và cỡ hạt trung bình tương ứng với từng dạng. Phần mềm được xây dựng dựa trên mã nguồn mở, tích hợp mô hình trí tuệ nhân tạo SAM2 giúp chỉnh sửa từng cục đá được phát hiện trong ảnh. Các kết quả cỡ hạt trung bình thu được từ phần mềm được so sánh với phân tích sàng truyền thống, chênh lệch dao động từ 5% đến 7% đối với riêng dữ liệu phân mảng hình ảnh, cho thấy tính khả thi của phần mềm trong việc trở thành một giải pháp giá rẻ, đáng tin cậy, có thể thay thế quy trình sàng.

Từ khóa: *Mức độ đập vỡ đất đá; phân phối cỡ hạt (PSD); hàm Swebrec; hàm Gate-Gaudin-Schumann; hàm Rossin-Rammler; SAM2; đập vụn; cỡ hạt trung bình; nổ phá.*

Received: 03/04/2025; Revised: 27/05/2025; Accepted for publication: 25/06/2025

❑